Comet 17P/Holmes: possibility of a CO driven explosion

Konrad J. Kossacki, Slawomira Szutowicz

Accepted Manuscript

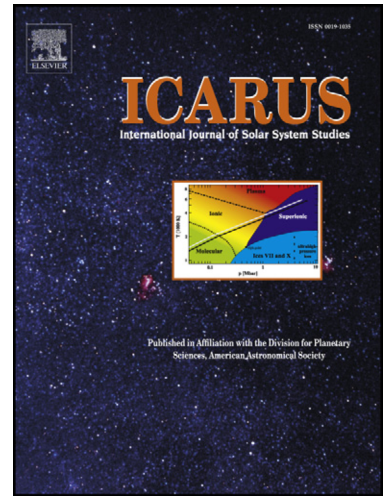

Comet 17P/Holmes: possibility of a CO driven explosion

Konrad J. Kossacki, Slawomira Szutowicz

PII: S0019-1035(11)00008-X
DOI: 10.1016/j.icarus.2011.01.007
Reference: YICAR 9686

To appear in: *Icarus*

Received Date: 7 July 2010
Revised Date: 31 December 2010
Accepted Date: 6 January 2011

Please cite this article as: Kossacki, K.J., Szutowicz, S., Comet 17P/Holmes: possibility of a CO driven explosion, *Icarus* (2011), doi: 10.1016/j.icarus.2011.01.007

Comet 17P/Holmes: possibility of a CO driven explosion

Konrad J. Kossacki

Institute of Geophysics of Warsaw University, Pasteura 7,02-093 Warsaw, Poland
E-mail: kjkossac@igf.fuw.edu.pl

Slawomira Szutowicz

Space Research Center of Polish Academy of Sciences, Bartycka 18a, 00-716, Warsaw, Poland

Number of pages (including figures):
Number of tables:
Number of figures:

Preprint submitted to Elsevier Science *12 January 2011*

Please send Editorial Correspondence to:
Konrad J. Kossacki
Institute of Geophysics of Warsaw University
Pasteura 7
02-093 Warsaw, POLAND
Tel: (48) 22 5546834
Fax: (48) 22 5546882
E-mail: kjkossac@igf.fuw.edu.pl

Proposed Running Head:
CO driven explosion

Abstract

This work is a continuation of our previous paper about brightening of Comet 17P/Holmes (Kossacki and Szutowicz, 2010). In that paper we presented results of simulations indicating that the nonuniform crystallization of amorphous water ice itself is probably not sufficient for an explosion. In the present work we investigate the possibility that the explosion is caused by a rapid sublimation of the CO ice leading to the rise of gas pressure above the tensile strength of the nucleus. We simulated evolution of a model nucleus in the orbit of Comet 17P/Holmes. The nucleus is composed of water ice, carbon monoxide ice and dust and has the shape of an elongated ellipsoid. The simulations include crystallization of amorphous ice in the nucleus, changes of the dust mantle thickness, and sublimation of the CO ice. In our model CO is mantling grains composed of dust and amorphous water ice. Orientation of the nuclear spin axis in space is the same as derived in Moreno et al. (2008) for Comet Holmes during recent brightening event. Hence, the angle between the orbital and the equatorial planes of the comet is $I = 95^o$, and the cometocentric solar longitude at perihelion is $\Phi = 210^o$. The calculations are performed for the south pole being the subsolar point close to time of the outburst. Our computations indicate, that the CO pressure within the comet nucleus can rise to high values. When the layer between the dust mantle and the crystallization front of the amorphous water ice is very fine grained, few microns in radius, the CO pressure within the nucleus can exceed 10 kPa. This value is the lowest estimate for the tensile strength of the nucleus of Comet Holmes (Reach et al., 2010). Hence, when the gas pressure reaches this value the nucleus may explode.

Key words: Comets, composition, Ices

1 Introduction

Comet 17P/Holmes underwent at least three massive explosions: in November 1892, in January 1893, and in late October 2007. The former two outbursts occurred about 144 and 216 days after perihelion passage, at the heliocentric distance of the comet 2.39 and 2.64 AU, respectively. The recent extreme jump of brightness with amplitude of over 14 magnitudes occurred at a distance of 2.44 AU from the Sun and 172 days after the last perihelion passage. In terms of the total mass of the dust emission, the 2007 explosion was more powerful than the two 1892 - 1893 outbursts combined (Sekanina, 2008). However, the apparent similarity of the above three events suggests the same trigger mechanism of the outbursts. The last extraordinary outburst of Comet Holmes in late October 2007 is still in the focus of interest of many investigators. Numerous observers investigated evolution of the cloud created during the explosion. Reach et al. (2010) distinguished three coma components: a shell, a 'blob' of ejecta containing separate filaments and a 'core' centered on the nucleus where the shell is due to small particles while the core and blob can be explained by larger particles. Ishiguro et al. (2010) estimated the lower limit of the ejected mass removed by the initial outburst for $4 \cdot 10^{10}$ kg (equivalent to a few meters thick surface layer of the nucleus) - presumably not only the dust mantle but also the pristine layer beneath the surface. Schleicher (2009) estimated a total amount of water ice and dust that was vaporized and emitted during four months of subsequent activity. The integrated water production implies that a mass of water ice of $2 \cdot 10^{10}$ kg corresponding to 0.2% of the total nucleus volume was vaporized, while a dust mass of $2 \cdot 10^{11}$ kg corresponding to at least 1% – 2% was released from the nucleus. Generally, the huge outburst of Comet Holmes is attributed to an internal explosive source of energy in the nucleus. In the literature are considered various exothermic chemical reactions involving free radicals or pockets of volatile gas stored beneath the surface (Altenhoff et al., 2009; Ishiguro et al., 2010; Reach et al., 2010; Schleicher, 2009; Sekanina, 2008). It should be also noted, that evolution of gas pressure within cometary nuclei and mechanisms for outbursts were investigated also in relations to other comets (e.g Prialnik and Bar-Nun, 1990; Huebner et al., 2006). The most obvious process, crystallization of the amorphous water ice, is highly exothermic, but may be too slow. In our previous paper (Kossacki and Szutowicz, 2010) we shown that crystallization of the amorphous water ice possibly present in cometary grains is probably not sufficient to lead to the observed explosion in Comet Holmes. Reach et al. (2010) considered heating of large scale closed subsurface pockets of amorphous ice and continuous rise of pressure until it can rupture the layer between a cavity and the surface of the nucleus. Schleicher (2009) speculated that a source of the explosive pressure could be a highly volatile ice, like CO or CO_2. The author argued that when the pressure became sufficient to destroy the subsurface layer, the boulders, chunks, and grains of dirt and water ice embedded within the matrix were explosively released into the coma (Schleicher, 2009). Indeed Stevenson et al. (2010) identified sixteen fragments of radii of 10-110 m ejected from the nucleus of Comet Holmes during its outburst. In the model proposed by Sekanina (2009) the CO trapped in amorphous water ice is released during the phase transition and subsequently superheated. According to the author the CO pressure rises until it reaches value needed to lift off a layer tens of meters thick. Sekanina (2009) has not explained why the CO vapor did not escaped the nucleus through the system of pores. We present more consistent approach, including sublimation of the CO ice and the diffusion of gas to space.

In the present work we intend to illustrate evolution of Comet Holmes after the previous explosion. During such an event a cometary nucleus can lose an outer layer several meters thick. This may significantly reduce the depth to the crystallization front of ice. Hence, we performed simulations for the model nucleus of the initial structure possible for the state after explosion: a dust mantle few centimeters thick; a layer composed of crystalline H_2O grains with mineral cores, about one meter thick; a layer of amorphous water ice grains with mineral cores, at least few meters; and interior of the nucleus, where in addition to H_2O ice some CO ice is present. Correct choice of the initial thickness of the dust mantle is difficult, because we start simulations after an explosion, when the dust mantle can quickly grow. A dust mantle few millimeter thick may form in days. When a comet approaches the Sun one orbital period after a global explosion it should be covered by a few centimeters thick layer of dust. Hence, we decided to consider the dust mantle initially a few centimeters thick. Thicknesses of the deeper layers are free parameters. In the interior of the nucleus, beneath the layer containing crystalline ice the cometary grains have two layered ice mantle. Just around the mineral core is the inner layer of ice, the crystalline H_2O ice, that in turn is covered by the layer of CO ice. Such structure can be formed, when the CO condenses after formation of the H_2O - mineral grains.

Our 2.5-D model of the nucleus includes evolution of the nucleus cohesion due to sintering of ice grains, crystallization of amorphous water ice, sublimation of CO ice mantling grains of amorphous water ice, recession of the surface, and evolution of the dust mantle. The latter includes increase of the dust thickness due to the sub-dust sublimation of ice, and local ejection of the dust when the vapor pressure exceeds a threshold value that is a free parameter. We look only for the conditions possibly leading to a rapid release of large amounts of energy, hence to an explosion. In our model energy is released in the nucleus at the crystallization front of ice. Thus, we look for the conditions leading to a rapid crystallization of water ice. In addition, we need conditions for slow diffusion of CO vapor through the near surface layer of the nucleus to space.

2 Description of the model

2.1 Basic properties

In this work we use a new version of our model, originally developed to investigate the evolution of Comet 46P/Wirtanen (Kossacki et al., 1999) and further significantly extended. The recent version was presented in Kossacki and Szutowicz (2010). Our model describes evolution of the temperature and cohesion of the material, crystallization of amorphous water ice, and emission of water to space. The nucleus is approximated by a two-axis elongated ellipsoid covered by a dust mantle of evolving thickness. The orbital elements are the same as for Comet 17P/Holmes. The orientation of the nucleus in space is described by angles between the orbital and equatorial planes of the comet. These angles are either constant, or may change their values after few orbital periods. In the current work they are assumed constant. The values of the angles are free parameters. Below we summarize basic properties of the model.

The nucleus is composed of mineral grains mantled by water ice, as well as mineral grains without ice. The latter form the dust mantle on the comet nucleus. The material beneath the dust mantle can evolve, while the dust layer has constant properties, except thickness. The ice mantling the grains can be: (i) crystalline everywhere in the nucleus (no amorphous water ice), or (ii) crystalline in a layer just beneath the dust mantle, and amorphous in the center of the nucleus. We note, that the ice mantling a grain is an ice shell around the mineral core, while the dust mantle is a layer of pure mineral grains at the surface of the comet nucleus. The former can be of a micron size, whereas the latter has thickness up to tens of centimeters. One more component of the nucleus is CO ice. To some depth any old cometary nucleus should be free of very volatile components such as CO. This should be expected as a consequence of the periodical surface warming of the nucleus and related sublimation of the volatile components. However, the depth where the CO ice is present is not known. This depth is determined not only by the initial nucleus structure, but also by the orbital history of the comet. Numerical simulations dealing with the chemical differentiation of a multi-component cometary nucleus in the orbit of Comet 46P/Wirtanen indicate recession of the CO sublimation front to a depth about 8 m during the first orbital period (Benkhoff, 2002). For a model nucleus in the orbit of 67P/Churyumov-Gerasimenko Huebner et al. (2006) have found, that the layer depleted of the CO ice is about 50 m after several revolutions around the Sun. In our work the initial depth to the CO sublimation front is a parameter.

When a comet approaches the Sun and the surface temperature rises, the ice starts sublimating beneath the dust mantle. The vapor partially escapes to space through the dust layer and partially migrates to the interior of the nucleus, where it condenses locally reducing porosity. Sublimation of ice may lead also to ejection of the dust mantle. In our model the dust mantle is removed when the vapor pressure beneath exceeds a threshold value that is a model parameter. One more process depending on warming of the surface is sintering of the ice-mineral grains.

The surface temperature is determined by variable insolation, thermal radiation into space, and heat transport through the dust mantle. The latter depends on the thermal properties of the dust layer and its thickness, as well as on the temperature beneath the dust. In the considered region the cometary surface is assumed to be free of topographic features. This means, we do not consider effects of shadowing, inclination of the surface, and absorption of the reflected light. The temperature at the bottom of the dust mantle depends on the heat transport at both sides, and the energy losses due to sublimation of ice. The flux of light absorbed at the surface depends on the local orientation of the surface, and on the current position of the Sun relative to the comet. The latter evolves due to the orbital motion and rotation of the comet. Variable illumination affects the surface temperature, hence the sublimation of ice beneath the dust mantle and the metamorphism of ice. The diffusion of heat in the nucleus depends on the temperature and properties of the nucleus material. Particularly important is the thermal conductivity. In this respect the considered layers are significantly different. The thermal conductivity is:
- very low in the dust mantle (small contact areas between the dust grains),
- high in the layer beneath the dust, composed of sintered grains of crystalline ice,
- very low beneath the crystallization front (very low thermal conductivity of the amorphous water ice, possibly small contact areas between grains).

The crystallization front is not only the boundary between the ice phases. It is also the boundary between the warm and cohesive outer layer and the cold and loose interior of the nucleus. The temperature jump and the thermal conductivity on the crystallization front have a significant influence on the rate of crystallization. The latter determines the rate of heat release and the related increase of the local temperature. This in turn enhances the sublimation of ices (mostly CO) and leads to an increase of the vapor pressure within the nucleus. Thus, very fast crystallization of ice may be able to cause an explosion due to the rise of the CO pressure.

2.1.1 Mathematical formulation

The model nucleus is covered by a dust mantle of evolving thickness. Immediately beneath the dust is a layer composed of ice-dust grains. These have mineral cores mantled by crystalline water ice. The interior of the nucleus is composed of mineral grains mantled by amorphous water ice, and starting from some depth also by CO ice.

The heat and vapor transport equations are solved 1D, in the radial direction. Horizontal transport is not calculated, because the horizontal scale is much larger than the thermal skin depth on the seasonal time scale. In this work, we solve the equations for the south pole of the nucleus being the sub-solar point at the beginning of the recent brightening event (Moreno et al., 2008). The basic equations are those for the diffusion of heat, the sintering of ice grains, and the crystallization of amorphous water ice. All formulas were described in our previous papers. The formula for the rate of ice crystallization can be found in Kossacki et al. (1999). The equation for the sintering of ice grains i.e. growth of the Hertz factor was described in Kossacki et al. (2006). The remaining formulas can be found in Kossacki and Szutowicz (2008).

At large depth the temperature remains constant. Thus, it is not needed to consider the whole nucleus. We perform simulations for the uppermost layer of the nucleus, of the thickness 20 meters, or 30 meters. Such a layer may be too thin to contain the dust emitted during the 2007 megaburst (see the Section 1). However, we do not simulate the explosion itself. Instead, we look for the possibility, that the process of crystallization rapidly accelerates. For this purpose it is enough, that the depth to the bottom of the considered layer of the nucleus is significantly larger than the depth to the crystallization front. In principle, thermal alterations to the nucleus composition could be possible at depths larger than considered in our work. However, in our model material beneath the crystallization front is loosely bounded and contains H_2O ice only in the amorphous form of extremely low thermal conductivity. In such case the crystallization front should be lower limit of the altered layer of the nucleus. We monitored structure of the model nucleus and would terminate calculations when the unaltered layer became thinner than 5 m. We performed simulations with resolution 2 cm. This is sufficient according to our numerical tests. When the surface recedes due to the sublimation of ice the number of grid points is reduced. The uppermost grid point is removed when the local position of the surface changes by a distance equal to the grid cell. The simulations are finished when the CO pressure exceeds the threshold value p_{expl} = 10 kPa. This value is the lower limit for the tensile strength of the outer part of the nucleus on the decameter scale (Reach et al., 2010). The time step is 0.25 minute when the distance to the Sun is smaller than 3 AU, and 0.5 minutes for larger heliocentric distances.

Initially, the cometary material has uniform temperature. The porosity and the Hertz factor (the ratio between the crossection of the neck between adjacent grains and of the crossection of a grain) are also uniform.

3 Parameters

Our model nucleus is a two-axial ellipsoid with semi-axes a= 2.1 km and b = c = 1.4 km. These values are close to these estimated for Comet Holmes by Snodgrass et al. (2006). The nucleus rotates with the rotational period 12 h with fixed orientation in space. The spin axis orientation is defined by two angles. The angle between the orbital and the equatorial planes of the comet is I = 95^o, and the cometocentric solar longitude at perihelion is $\Phi = 210^o$. The latter is the angle measured from the vernal equinox of the comet in the sense of increasing true anomaly to the sub-solar meridian at perihelion. For such orientation the south polar region (the source of the main "jets" of the emission from Comet Holmes) was illuminated close to time of the outburst (Moreno et al., 2008). We solve the heat and vapor transport equations for the southern pole of the nucleus.

In our simulations we assume that the initial (i.e. after explosion) structure of the nucleus is the following:
(a) dust mantle of the thermal conductivity k_d = 20 - 150 mW m^{-1} K^{-1} (thickness: 4 cm),
(b) layer composed of crystalline H_2O grains with mineral cores (thickness: 0.5 m),
(c) layer of amorphous water ice grains with mineral cores (thickness: 3.5 m, 9.5 m, or 19.5 m), and
(d) interior of the nucleus, where the water ice grains are additionally mantled by CO ice. In the result we locate the initial sublimation front of the CO ice, z_{CO} at a depth of 4 m, 10 m or 20 m.

The nucleus material underlying the dust mantle is described by: the volume fractions of the components; (v_m - of the mineral cores, v_{H2O} - of the H_2O ice, and v_{CO} - of the CO ice), the Hertz factor h, the radii of grains and pores $r_g = r_p$, and the tortuosity of pores τ. The volume fractions are normalized to the total volume including pores. Hence, they can be related to the porosity ($\psi = 1 - v_m - v_{H2O} - v_{CO}$). The volume v_m of the mineral cores of grains is constant (does not evolve). The volume fraction v_{H2O} of H_2O ice evolves: slowly increases from the initial value $v_{H2O,0}$ due to condensation of the H_2O vapor migrating toward the center of the nucleus. The volume fractions v_m, $v_{H2O,0}$, and $v_{CO,0}$ are free parameters.

The native CO abundance relative to water varies from comet to comet. It should be also noted, that the thermal evolution of a cometary nucleus leads to the formation of an inhomogeneous structure (Huebner and Benkhoff, 1999). Hence, the composition observed in a coma may be significantly different than the average composition of a nucleus. In the Oort cloud comets the molecular concentration of CO relative to H_2O is 0.4 - 17% (Bockelée-Morvan et

Table 1
The volume fractions of the nucleus components and the model densities.

model	v_m	$v_{H2O,0}$	$v_{CO,0}$	density below the CO sublimation front [$\mathrm{kg\,m^{-3}}$]	initial molecular ratio CO:H_2O	ratio dust to water
Very high dust content	0.226	0.094	0.03	600	26%	5.00
High dust content	0.170	0.250	0.03	641	10%	1.41
High density	0.170	0.266	0.03	656	9%	1.33
Moderate density	0.135	0.266	0.01-0.1	557–658	3% - 28%	1.05
Low dust content	0.100	0.266	0.03	511	9%	0.78

al., 2005). For Comet Holmes the relative abundance of carbon monoxide was 14 ± 4 % six days after the outburst (Salyk et al., 2007). At the time of the peak production rate the amount of water in the coma was $7 \cdot 10^{35}$ molecules (Sekanina, 2008). The maximum possible contents of CO ejected impulsively from the nucleus was estimated to be of $7 \cdot 10^{32}$ molecules (Drahus, private information). However, one should note that water contents reported by Sekanina (2008) was mostly created in the coma from ice grains and these grains were rejected from the CO depleted subsurface layers in the outburst time. Hence, this amount of water can not be used to calculate the initial relative CO content in the nucleus at large depths (beneath the sublimation front of CO ice).

In our work the volume fraction of the CO ice v_{CO} is zero above the receding sublimation front, and $v_{CO,0} = 0.01 - 0.09$ at larger depths. The corresponding range of the molecular ratio CO:H_2O is 3% - 28%. The volume fraction of mineral component is v_m = 0.1 - 0.2256, and the initial volume fraction of water is $v_{H2O,0}$ = 0.094 - 0.2655. In respect of the density we distinguish the following models: Very high dust content, High dust content, High density, Moderate density, and Low dust content. The investigated dust-to-water mass ratio ranges between 0.8 and 5. Conversion of this ratio to the number density of the dust grains in coma is difficult for several reasons. Among them are: possible fragmentation of grains, and production of dust from the surface not considered in our work. There are reports of very large dust-to-gas ratio for post-outburst Holmes. Schleicher (2009) concludes that Comet Holmes is about five times dustier than other comets with similar perihelia. Sekanina (2008) also estimates the dust-to-water mass production rate ratio for ≤ 5. Thus we include the case of very high dust-to-water ratio in the Very high dust model.

The initial compositions and densities are given in Table 1.

The initial Hertz factor is 0.01 - 0.25. The higher value means higher cohesivity of the nucleus. The radii of grains and pores are 0.002 - 0.20 mm, and tortuosity of the pores is $\sqrt{2}$. In reality, the radii of grains and pores can change slightly as the migrating vapor condenses. However, these changes are not so significant as the changes of grain-to-grain contact areas resulting from the activity of sintering mechanisms.

The dust mantle is locally removed when the vapor pressure beneath the mantle exceeds the threshold pressure, $p_{dust} = 10$ Pa. Calculations for higher values of p_{dust} give the same effect as for 10 Pa (Kossacki and Szutowicz, 2010). The threshold pressure of CO vapor p_{expl} at the CO sublimation front, yielding explosion i.e rejection of the whole material above, is 10 kPa. The model parameters are summarized in Table 2.

Table 2
Model parameters

Parameter	Symbol	Unit	Value
Albedo, emissivity	A, ϵ		0.04, 0.97
Density of the mineral cores of the grains	ϱ_m	[kg m^{-3}]	2078
Thermal conductivity of the mineral cores	λ_m	[W m^{-1} K^{-1}]	3.1
Initial volume fraction of H_2O ice	$v_{H2O,0}$		0.094 - 0.2655
Initial volume fraction of CO ice	$v_{CO,0}$		0.01 - 0.09
Volume fraction of the mineral component	v_m		0.1 - 0.2256
Bulk density of the nucleus above the CO sublimation front	ϱ	[kg/m^2]	474 - 620
Molecular fraction CO:H_2O			3% - 28%
Tortuosity	τ		$\sqrt{2}$
Grain/pore radius in the ice-dust medium	$r_g = r_p$	[mm]	0.002 - 0.02
Pore radius in the dust layer	r_d	[mm]	$2r_g$
Thermal cond. of the dust layer	λ_d	[W m^{-1} K^{-1}]	0.02 - 0.15
Specific heat of dust layer	c_d	[J kg^{-1}K^{-1}]	1200
Porosity of the dust layer	ψ_d		0.73
Threshold vapor pressure yielding local rejection of the dust mantle	p_{dust}	[Pa]	10
Threshold vapor pressure yielding explosion at the CO sublimation front	p_{expl}	[kPa]	10
Initial depth of the CO sublimation front	z_{CO}	[m]	4 - 20
Initial temperature	T	[K]	20
Initial Hertz factor	h_o		0.01 - 0.25
Other parameters:			
The spin axis orientation:			
Obliquity	I	[deg.]	95^o
Solar longitude at perihelion	Φ	[deg.]	210^o
Perihelion distance	q	[AU]	2.053
Eccentricity	e		0.432
Orbital period	P	[year]	6.88

4 Results

All calculations are performed for the region located at the southern pole of the nucleus.

In Fig. 1 we shown the results of simulations for the moderate density model nucleus with a thick layer depleted in CO ice. The initial position of the CO sublimation front is 10 meters beneath the surface. We drawn profiles of: (i) pressure of the CO vapor versus time, and (ii) current position of the local surface versus time. For the CO pressure we plotted peak values for the consecutive equal intervals, 100 per orbital period. The model parameters are: the volume fractions of the mineral component $v_m = 0.1345$, of the water ice $v_{H2O,0} = 0.2655$, and of the carbon monoxide ice $v_{CO,0} = 0.03$; the thermal conductivity of the dust mantle $k_d = 100$ mW m^{-1} K^{-1}; the threshold pressure of H_2O vapor yielding local rejection of the dust mantle $p_{dust} = 10$ Pa; the threshold pressure of CO vapor $p_{expl} = 10$ kPa; the size of grains $r_g = 0.002 - 0.020$ mm, the initial Hertz factor $h_0 = 0.10$ - 0.25. During the first orbital period the CO pressure remains very low. It starts growing when the comet approaches the Sun in the following returns. When the grains are very fine, of the radius 2 microns, the CO pressure quickly rises during the third return of the comet and almost immediately reaches the threshold value 10 kPa. This happens 280 days or 290 days after perihelion passage depending on the assumed value for the initial Hertz factor $h_0 = 0.25$ or $h_0 = 0.10$, respectively. When the cometary grains are 20 microns in radius the CO pressure changes relatively slowly. The peak pressure increases from one orbital period to another, but not enough to reach the threshold value, and tends to stabilize. Hence, an explosion is not likely when the grains are 20 microns in radius. Comparison of the profiles of p_{CO}, and of the current position of the surface versus time shows, that the gas pressure at the CO sublimation front reaches the critical value p_{expl} when the surface of the nucleus is about 6.5 m lower than initially. This value corresponds the distance z_{CO} from the nucleus surface to the sublimation front of CO about 3.5 m.

In the upper panel of Fig. 2 we shown the calculated temperature at the CO sublimation front beneath the surface. The parameters are the same as for Fig. 1. The values are plotted every 1/100 of the orbital period, each time for the current sublimation front of CO ice. As the CO sublimes, the grid point corresponding to the current position of the sublimation front changes. Hence, one profile of the temperature versus time contains values from different grid points, what makes it rough. We have smoothed the profile by removing local minimums. For the smallest grains of $r_g = 2$ microns the temperature quickly rises from the initial value 20 K to the value about 63 K. The latter corresponds to the phase equilibrium pressure 10 kPa, hence to the explosion. When the grains are larger, $r_g = 20$ microns, the temperature maximum is only a few degrees lower. However, this difference is sufficient to keep the CO pressure low. In Fig. 2 (middle panel, and lower panel) we shown calculated profiles of temperature in the model nucleus versus depth. In addition we plotted also fraction of the crystalline phase in H_2O ice versus depth (lower panel). The latter is to show location of the crystallization front. The results are for two cases: the nucleus is composed of very fine grains ($r_g = 2$ microns), and moderately fine grains ($r_g = 20$ microns). Both profiles are drawn for the time 280 days after perihelion passage. In the case of the very fine grains model the temperatures correspond to the state just before explosion. When the grains are moderately fine the explosion is not predicted. In each case the profile is flat above the crystallization front and very steep just beneath it. This is due to a jump of the thermal conductivity of the material at the crystallization front. During crystallization the thermal conductivity of ice changes from $7.110^{-8}\ T$ to $567/T$. Simultaneously, the temperature rises due to release of the latent heat and the contact areas between adjacent grains start to increase due to the sintering process. Finally, the thermal conductivity increases by few orders of magnitude. The sublimation of CO ice is possible only at depth where the temperature is significantly higher than the initial temperature 20 K. Hence, CO ice sublimes in the area of high temperature gradient. Inaccuracy of the calculated temperature can result in noticeable inaccuracies of the calculated CO pressure and of the time when the gas pressure exceeds the threshold value.

Fig. 3 is analogous to the upper panel of Fig. 1. The differences are: the initial depth z_{CO} from the surface to the sublimation front of CO is only 4 meters, and k_d has two values (20 mW m^{-1} K^{-1}, and 100 mW m^{-1} K^{-1}). The remaining model parameters are the same as for Fig. 1. The CO vapor at the sublimation front can rise to threshold pressure p_{expl} yielding explosion only when the nucleus is composed of very fine grains. This result is the same as in the case of high initial depth z_{CO} of the sublimation front of CO. This what is different is the time of explosion. When $z_{CO} = 10$ m (Fig. 1) the model nucleus explodes within the third orbital run, about 285 days after perihelion passage. For $z_{CO} = 4$ m (Fig. 3) explosion is predicted already for the first approach to the Sun, 160 - 220 days after perihelion depending on the initial Hertz factor and the dust mantle conductivity.

In Fig. 4 we shown results obtained for a nucleus of different mass ratios dust-to-water. The thermal conductivity of the dust mantle $k_d = 100$ mW m^{-1} K^{-1}. In the upper panel of Fig. 4 are shown results for the model Very high dust content (dust-to-water ratio = 5). The middle panel of Fig. 4 shows results for the High dust content model (dust-to-water ratio = 1.4). The volume fraction of dust $v_m = 0.17$ is about 25% higher than in our moderate density model. In the lower panel of Fig. 4 we shown results obtained for the Low dust content model (dust-to-water ratio = 0.8), with $v_m = 0.1$, about 20% lower than in our moderate density model (see Fig. 1).

For all considered mass ratios dust-to-water the pressure of CO vapor can rise to the threshold value p_{expl} only when the nucleus is composed of very fine grains. The time of explosion significantly depends on the water ice content in the nucleus. When the concentration of dust is very high, dust-to-water = 5, but the volume fraction of water ice is about 0.1, explosion is predicted already for the first or the second orbital run about 80 - 130 days after perihelion. For the High dust content model the time of explosion is 300-320 days after perihelion of the third orbital run. The delay of the explosion relative to the perihelion is again smaller for the nucleus poor in dust. Then the CO pressure reaches the explosive value about 190 days ($h_0 = 0.25$) and about 210 days ($h_0 = 0.10$) after perihelion.

The Very high dust content model, mass ratio dust:water = 5, predicts explosion much closer to perihelion than the other models considered in our paper. When the nucleus is composed of very small grains, $r_g = 0.002$mm, and is moderately cohesive, $h_0 = 0.10$ - 0.25 the Very High dust content model predicts rise of the CO pressure to the critical value 10 kPa less than 150 days after perihelion. For the same parameters models with the dust:water ratio = 0.8 - 1.4, predict explosion 200 - 400 days after perihelion. It should be noted, that the Very high dust content model is characterized by very low water content, only 16% of the mass. In the remaining models the water ice accounts for 43% - 52% of the total mass of the nucleus.

We investigated also influence of the initial position of the CO sublimation front. For this purpose we performed additional simulations using the High dust content model with the initial depth to the CO sublimation front increased from 10 m to 20 m. The predicted time of explosion in days after perihelion was only slightly changed. However, the number of orbital revolutions before explosion increased by five, from 2 to 7.

In addition we investigated the role of the abundance of CO ice. For this purpose we have modified the model considered in the Fig. 1 ($v_m = 0.1345$, $v_{H2O,0} = 0.2655$, $v_{CO,0} = 0.03$, $k_d = 100$ mW m^{-1} K^{-1}, $r_g = 0.002$ mm, and $h_0 = 0.25$) to investigate the influence of the volume fraction of CO. The simulation of the nucleus with different $v_{CO,0}$ shown that the concentration of the CO ice has very small influence on the time of explosion. The time after perihelion, when the CO pressure reaches the explosive value is 280 days for values of $v_{CO,0}$ within the range 0.01 - 0.09, i.e. when the molecular ratio CO:H_2O is 3% - 28%.

In Table 3 we summarize all simulated models and calculated time of the explosion (in days after perihelion) when the CO pressure reached the explosive value. In the subsequent columns are shown: the initial position of the CO sublimation front, z_{CO}; the size of grains, r_g; the volume fractions of the CO ice, v_{CO}; the initial Hertz factor, h_0; the thermal conductivity of the dust mantle, k_d; the orbital revolution in which the outburst occurred, N; the time of outburst. The cases when the calculated time of explosion in days after perihelion differs of the observed one, 172 days, by less than 10 days are marked with bold. The cases when the CO pressure remains low (no explosion) are also listed.

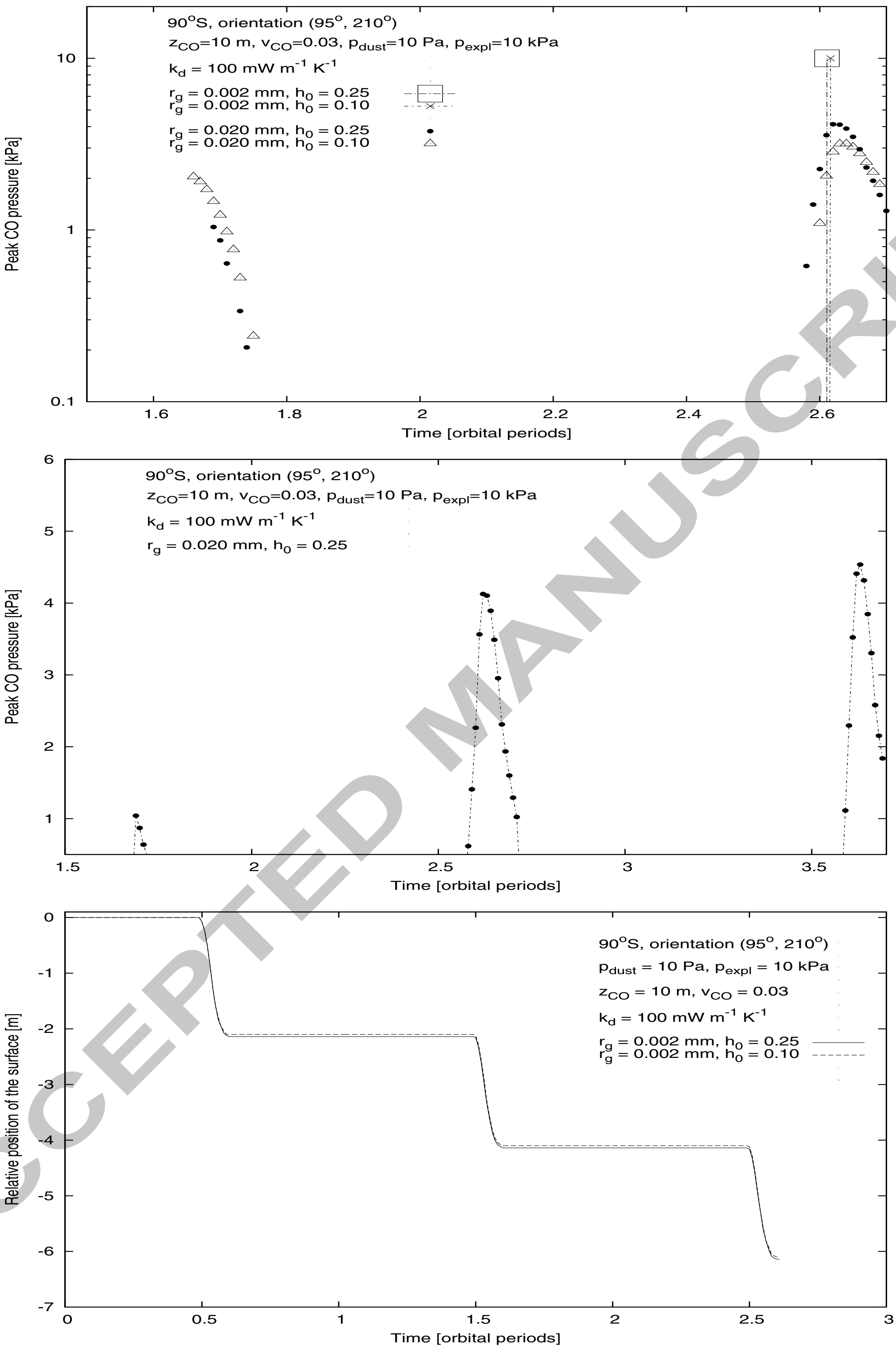

Fig. 1. Results for the model nucleus with the CO sublimation front located initially 10 meters beneath the surface at the south pole. **Upper panel, and middle panel**: the gas pressure at the CO sublimation front; plotted are the highest values reached in the consecutive equal intervals, 100 per orbital period. **Lower panel**: position of the surface versus time; the position is zero at the beginning of the simulations. Upper panel: the model grains are of radii 0.002 and 0.020 mm, and the initial Hertz factor is 0.1 and 0.25. Middle panel: $r_g = 0.020\,\text{mm}$, $h_0 = 0.25$. Lower panel: $r_g = 0.002\,\text{mm}$, $h_0 = 0.01$ - 0.25.

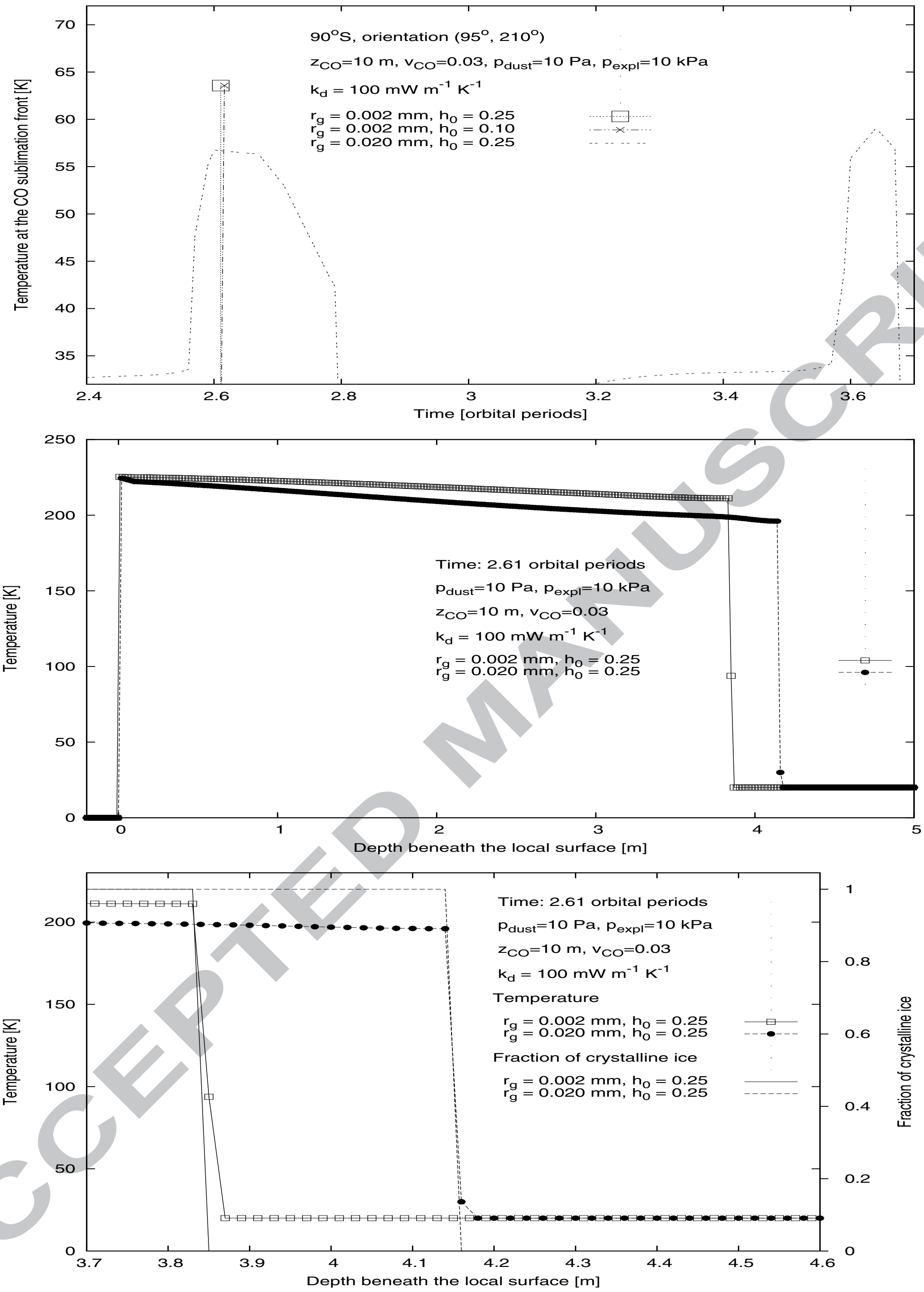

Fig. 2. Temperature in the model nucleus. The model parameters are: $k_d = 100$ mW m^{-1} K^{-1}; $p_{dust} = 10$ Pa, $p_{expl} = 10$ kPa; $r_g = 0.002 - 0.020\,$mm; and h_0 is 0.10 - 0.25. **Upper panel:** Temperature at the CO sublimation front beneath the south pole versus time. The profiles correspond to the profiles of the CO pressure shown in Fig. 1. **Middle panel and lower panel:** Temperature versus depth at a fixed time for two cases: $r_g = 0.002\,$mm, and $r_g = 0.020\,$mm. In the former case the chosen time corresponds to the state just before explosion. The points are drawn every 2 cm. In the lower panel we shown additionally profiles of the crystalline phase in H_2O ice versus depth.

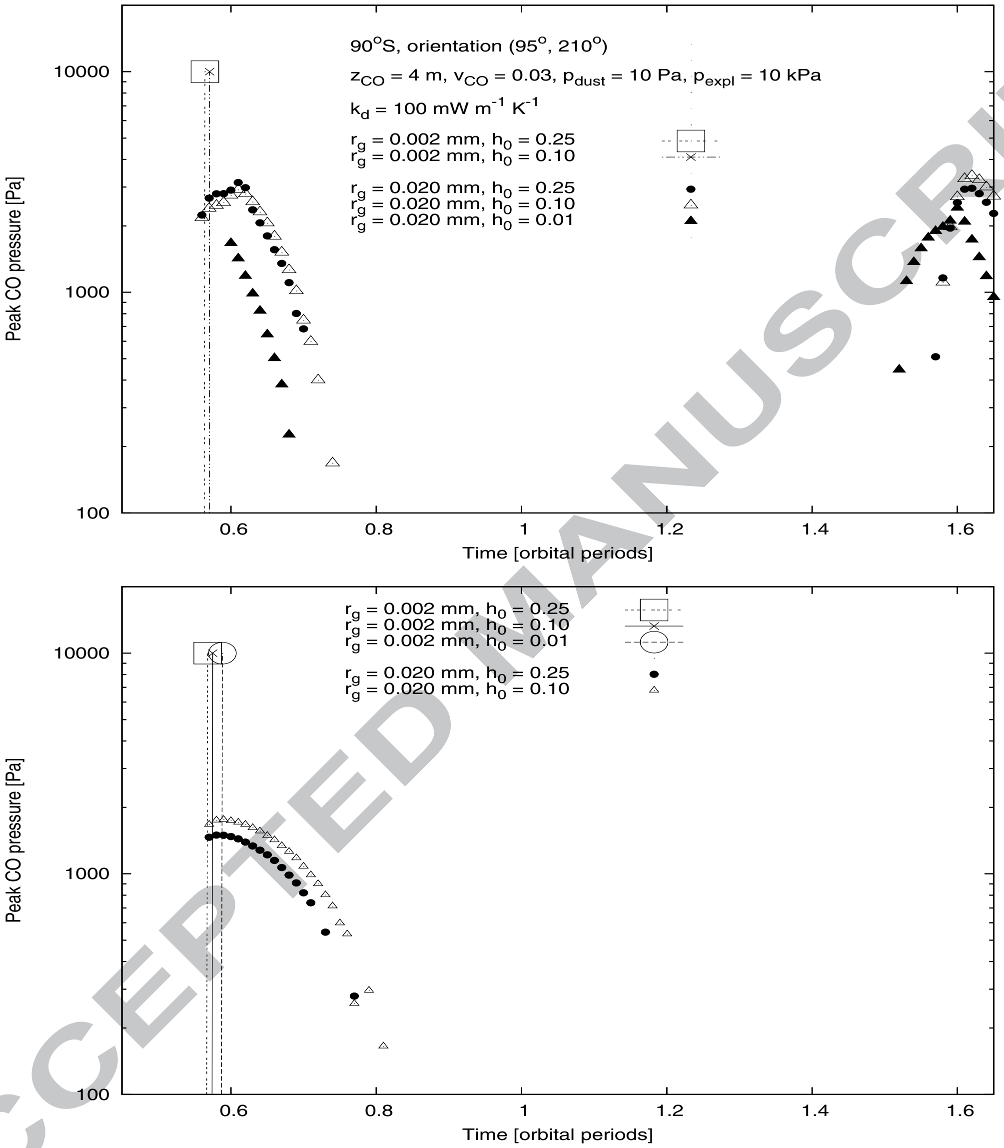

Fig. 3. Gas pressure at the CO sublimation front beneath the south pole. The profiles are analogous to these in the upper panel of Fig. 1. The differences are: the initial depth z_{CO} from the surface to the sublimation front of CO is 4 meters instead of 10 meters, and k_d has two values (100 mW m^{-1} K^{-1}, and 20 mW m^{-1} K^{-1}). The results for 100 mW m^{-1} K^{-1} we shown in the upper panel, while these for 20 mW m^{-1} K^{-1} in the lower panel.

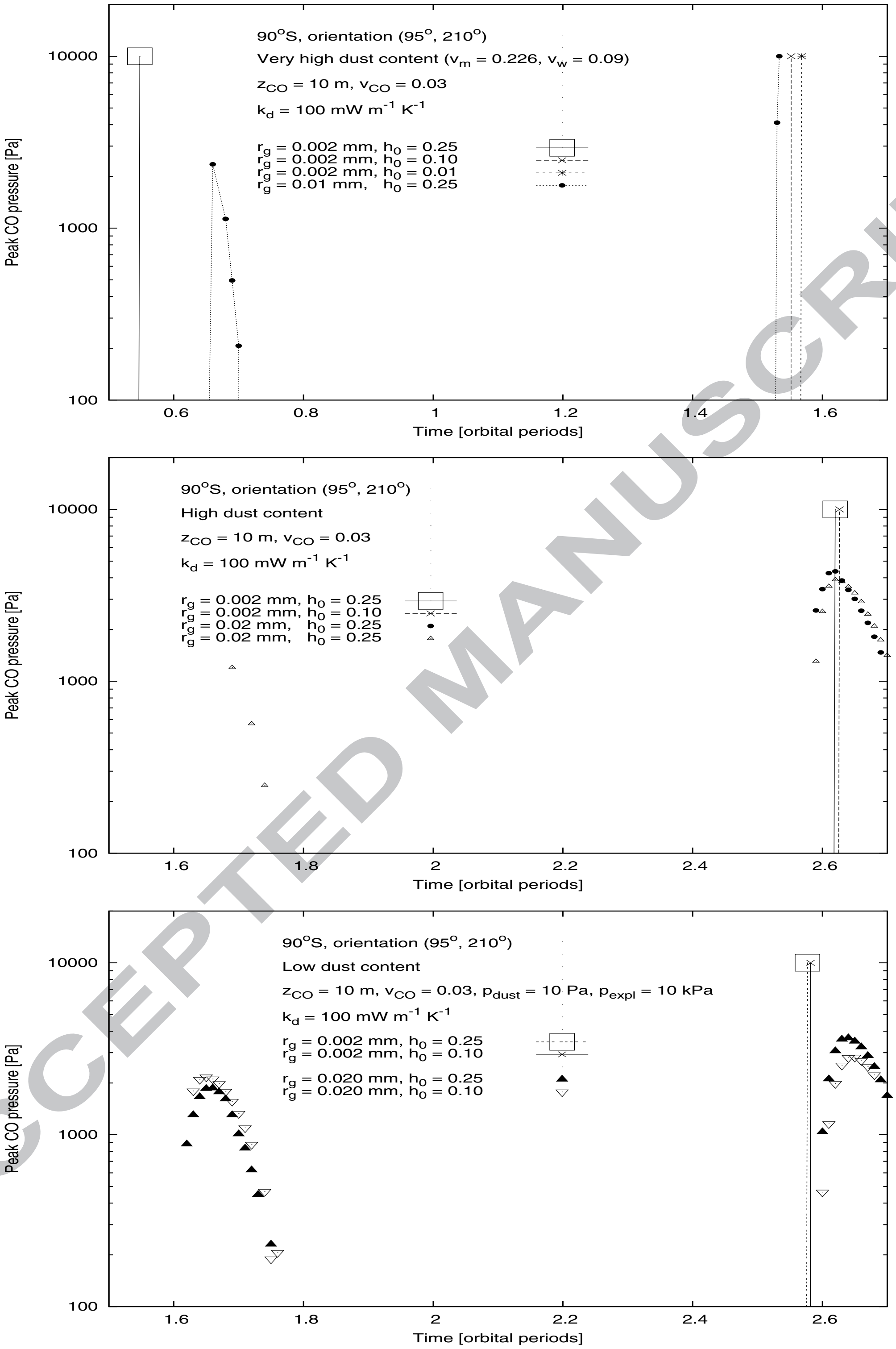

Fig. 4. The same as in the upper panel of Fig. 1 but for different contents of dust in the nucleus: Very high dust content (upper panel), High dust content (middle panel), and Low dust content (lower panel).

Table 3
The calculated time of explosion in days after perihelion passage of the N-th orbital revolution.

z_{CO} [m]	r_g [mm]	v_{CO}	h_0	k_d [mW m^{-1} K^{-1}]	N	Time [days after perihelion]
Very high dust content			($\varrho = 600$ kg m^{-3}, dust:ice = 5)			
10	0.002	0.03	0.25	100	1	120 (Fig.4)
10	0.002	0.03	0.25	20	2	**160**
10	0.002	0.03	0.10	100	2	130 (Fig.4)
10	0.002	0.03	0.01	100	2	**170** (Fig.4)
10	0.01	0.03	0.25	100	2	90 (Fig.4)
High dust content			($\varrho = 641$ kg m^{-3}, dust:ice = 1.4)			
10	0.002	0.03	0.25	100	3	300 (Fig.4)
10	0.002	0.03	0.10	100	3	320 (Fig.4)
20	0.002	0.03	0.25	100	8	260
10	0.02	0.03	0.25	100		— (Fig.4)
High density			($\varrho = 656$ kg m^{-3}, dust:ice = 1.3)			
10	0.002	0.03	0.25; 0.10	100	3	390
10	0.002	0.03	0.25	20		—
10	0.004	0.03	0.25	100	3	270
10	0.008	0.03	0.25	100	5	310
Moderate density			($\varrho = 557$-658 kg m^{-3}, dust:ice = 1.1)			
10	0.002	0.01	0.25	100	3	280
10	0.002	0.03	0.25	100	3	280 (Fig.1)
10	0.002	0.03	0.25	20	3	250
10	0.002	0.03	0.10	100	3	290 (Fig.1)
10	0.002	0.09	0.25	100	3	280
10	0.020	0.03	0.25; 0.10	100		— (Fig.1)
4	0.002	0.03	0.25	100	1	**160** (Fig.3)
4	0.002	0.03	0.25	20	1	**170** (Fig.3)
4	0.002	0.03	0.10	100	1	**180** (Fig.3)
4	0.002	0.03	0.10	20	1	190 (Fig.3)
4	0.002	0.03	0.01	20	1	220 (Fig.3)
4	0.02	0.03	0.25; 0.10; 0.01	100		— (Fig.3)
4	0.02	0.03	0.25; 0.10	20		— (Fig.3)
Low dust content			($\varrho = 511$ kg m^{-3}, dust:ice = 0.8)			
10	0.002	0.03	0.25	150	3	220
10	0.002	0.03	0.25	100	3	190 (Fig.4)
10	0.002	0.03	0.10	150	3	200
10	0.002	0.03	0.10	100	3	210 (Fig.4)
10	0.002	0.03	0.01	150	3	230
10	0.02	0.03	0.25; 0.10	100		— (Fig.4)
10	0.02	0.03	0.25; 0.10	20		—

5 Discussion and conclusions

In our previous paper about Comet Holmes (Kossacki and Szutowicz, 2010) we shown, that crystallization of H_2O ice itself is probably not sufficient to cause large explosion of the nucleus of the comet. In that work we simulated evolution of a model nucleus to study the influence of changes in the orientation of the nuclear spin axis on the rate of ice crystallization in the nucleus. Our calculations indicated that the crystallization process accelerates after the changes in the orientation. However, a large jump of the crystallization front of about 8 m at high latitudes in the southern hemisphere was predicted only for large changes in the orientation of the nuclear spin axis. While, small changes in the nucleus orientation usually lead to a similar large movement of the crystallization front only in the northern hemisphere. In all considered cases our model did not predict an increase in the water vapor pressure sufficient to cause a large-scale explosion. In our present work we investigated another possible mechanisms for the explosion of a cometary nucleus, namely rise of the gas pressure within nucleus due to fast sublimation of the CO ice. We considered model nucleus similar to the nucleus of Comet Holmes. Our simulations indicate, that the nucleus of Comet Holmes may explode due to the sublimation of CO ice in the southern polar region (the region exposed to solar radiation close to the time of outburst). However, the explosion is possible only when the cometary material is very fine grained, $r_g < 0.01$ mm. This result is in agreement with the general prediction, that high gas pressure can build up in fine-grained nuclei (e.g. Huebner et al., 2006).

The exact time, when our model nucleus explodes significantly depends on several parameters: the nucleus density, the size of grains, thermal conductivity of the dust mantle, the initial degree of the sintering (h_0), and on the initial depth of the CO sublimation front. Our simulations show that an agreement between the calculated time of the explosion in days after perihelion with the observed time of megaburst of Comet Holmes, about 170 days, is possible for different compositions of the model nucleus.

The calculated time of outburst exhibits a complex dependence on the nucleus properties. Particularly important are two effects: (i) for a nucleus of low cohesivity, composed of small grains the outburst happens further from the perihelion passage than for a cohesive coarse-grained nucleus, and (ii) the time of the outburst is highly influenced by the content of dust in the nucleus. Our numerical simulations for the Very high dust content model (dust-to-water ratio =5), predict the outburst much closer to perihelion than other models considered in the paper.

In our model cometary grains located beneath the depleted subsurface layer contain some CO ice. It is not known whether the cometary grains can contain

CO trapped only within amorphous water ice, or also as the separate ice. We considered the grains composed of mineral cores mantled by two ices: H_2O ice just on the core and CO ice on H_2O ice. This approach may underestimate the production rate of the gaseous CO. However, the tensile strength of the upper layer of the nucleus can be an order of magnitude higher than considered in our work (Reach et al., 2010) making explosion very unlikely. Possibly the tensile strength can be occasionally reduced due to formation of cracks. This may help to understand, why huge explosions of comet nuclei are so exceptional.

Acknowledgments

This work was partially supported by the Polish Ministry of Education and Science (grant 4036/B/H03/2010/39). We thank anonymous referees for their valuable comments. We thank also M. Drahus for his remarks.

References

A'Hearn, M. F., Belton, M.J.S., Delamere, W.A., and 31 colleagues, 2005. Deep Impact: Excavating Comet Tempel 1. Science 310, 258-264.

Altenhoff, W. J., E. Kreysa, K. M. Menten, A. Sievers, C. Thum, and A. Weiss, 2009. Why did Comet 17P/Holmes burst out? Nucleus splitting or delayed sublimation? A&A 495, 975-978.

Benkhoff, J., 2002. The emission of gas and dust from comets. Adv. Space Res. 29, No. 8, 1177-1186.

Bockelée-Morvan, D., Crovisier, J., Mumma, M.J. and Weaver, H.A., 2005. The Composition of Cometary Volatiles. In: Festou, M.C., Keller, H.U., Weaver, H.A. (Eds.), Comets II. Univ. of Arizona Press, Tucson, pp. 391-423.

Huebner, W. F., Benkhoff, J., 1999. From coma abundances to nucleus composition. Space Sci. Rev. 90, 117-130

Huebner, W.,F., Benkhoff, J. Capria, M.-T., Coradini, A.; de Sanctis, Ch., Orosei, R., Prialnik, D., 2006. Heat and Gas Diffusion in Comet Nuclei. Published for The International Space Science Institute, Bern, Switzerland, by ESA Publications Division, Noordwijk, The Netherlands.

Ishiguro, M., Watanabe, J., Sarugaku, Y., Ootsubo, T., Kuroda, D., Honda, M., Miyata, T., Yanagisawa, K., Mito, H., Fukushima, H., Niwa, T., Sakamoto, M., Narusawa, S., and Akisawa, H., 2010 2007 Outburst of 17P/Holmes: The Albedo and the Temperature of the Dust Grains. Astroph. J., 714, 1324-1333.

Kossacki, K.J., Szutowicz, S., and Leliwa-Kopystyński, J., 1999. Comet 46P/Wirtanen: Evolution of the Subsurface Layer. Icarus 142, 202-218.

Kossacki, K.J., Leliwa-Kopystynski, J., and Szutowicz, S., 2006. Evolution of depressions on Comet 67P/Churyumov Gerasimenko: Role of ice metamorphism. Icarus, 184, 221-238.

Kossacki, K.J., and Szutowicz, S., 2008. Comet 9P/Tempel 1: sublimation beneath the dust cover. Icarus 195, 705-724.

Kossacki, K.J., and Szutowicz, S., 2010. Crystallization of ice in Comet 17P/Holmes: Probably not responsible for the explosive 2007 megaburst. Icarus 207, 320-340.

Moreno, F., Ortiz, J.L., Santos-Sanz, P., Morales, N., Vidal-Nunez, M.J., Lara, L.M., and Gutierrez, P.J., 2008. A model of the early evolution of the 2007 outburst of Comet 17P/Holmes. Astrophys. J. 677, L63 - L66

Prialnik, D., and Bar-Nun, A., 1990. Gas release in comet nuclei. Astrophys. J. , 363, 274-282.

Reach, W. T., Vaubaillon, J., Lisse, C. M., Holloway, M., Rho, J., 2010. Explosion of Comet 17P/Holmes as revealed by the Spitzer Space Telescope. Icarus, 208, 276-292.

Salyk, C., Blake, G. A., Mumma, M. J., Bonev, B. P., Disanti, M. A., Villanueva, G. L., Radeva, Y., Magee-Sauer, K., Gibb, E. L., 2007. Comet 17P/Holmes. IAUC 8890, 1.

Schleicher, D. G., 2009. The Long-Term Decay in Production Rates Following the Extreme Outburst of Comet 17p/Holmes. Astrophys. J., 138, 1062-1071.

Schmitt, B., Espinasse, S., Grim, R.J.A., Greenberg, J.M., and Klinger, J., 1989. Laboratory Studies of Cometary Ice Analogues. Physics and Mechanics of Cometary Materials, ESA SP-302, 65-69

Sekanina, Z., 2008. Exploding Comet 17P/Holmes. Intern. Comet Quarterly 30, No.1, 3–28

Sekanina, Z., 2009. Crystallization of Gas-Laden Amorphous Water Ice, Activated by Heat Transport to its Subsurface Reservoirs, as Trigger of Huge Explosions of Comet 17P/Holmes. ICQ 31, 99-124.

Snodgrass, C., Lowry, S.C., and Fitzsimmons, A., 2006. Photometry of cometary nuclei: rotation rates, colors and a comparison with Kuiper Belt Objects. Mon. Not. R. Astron. Soc. 373, 1590–1602

Stevenson, R., Kleyna, J., Jewitt, D., 2010. Transient Fragments in Outbursting Comet 17P/Holmes. Astron. J., 139, 2230-2240.

ACCEPTED MANUSCRIPT